Journal of Applied Physics ARTICLE pubs.aip.org/aip/jap

Electron mobility of heavily doped semiconductors including multiple scattering by ionized impurities

Cite as: J. Appl. Phys. **134**, 075701 (2023); doi: 10.1063/5.0165201
Submitted: 27 June 2023 · Accepted: 27 July 2023 ·
Published Online: 15 August 2023

D. L. Rode[1] and John S. Cetnar[2,a)]

AFFILIATIONS

[1]Department of Electrical Engineering, Washington University, St. Louis, Missouri 63130, USA
[2]Air Force Research Laboratory—Sensors Directorate, Wright-Patterson Air Force Base, OH 45433, USA

[a)]**Author to whom correspondence should be addressed:** john.cetnar.1@us.af.mil

ABSTRACT

A theoretical treatment of the multiple scattering problem for electrons in heavily doped semiconductors is developed for the purpose of resolving a long-standing discrepancy between theory and experiment on electron transport in semiconductors and semimetals. The scattering *strength* term in the traditional Brooks–Herring formula for ionized impurity scattering is modified to take into account the effect of the spatial proximity of ionized donors leading to an additional scattering term proportional to the *cube* of ionized impurity concentration, whereas the Brooks–Herring theory varies strictly linearly with the ionized impurity concentration. Comparisons between theory and experiment for GaAs, GaN, ZnO, and α-Sn are presented, showing significant improvement overall. In some cases, improvements greater than an order of magnitude are achieved. The agreement between theory and experiment for heavily doped ZnO over the temperature range of 21–322 K is within about 1%, depending on temperature.

Published by AIP Publishing. https://doi.org/10.1063/5.0165201

I. INTRODUCTION

It is well-known, by comparisons between theory[1–8] and experiment,[9–14] that theoretical calculations of electron mobility by solution of the Boltzmann transport equation using the Born approximation for electron scattering by ionized impurities show considerable disagreement with experiment. For heavily doped semiconductors, the disagreement between theory and experiment amounts to about 40%–80%, the theoretical electron mobility being too large. Initially, this discrepancy was thought to be due to either multiple scattering of electrons by dopant impurities, or compensation of donors by ionized acceptor impurities, and especially in low-doped cases, the latter is arguably the correct interpretation. However, there has arisen an overweening reliance on dopant compensation to explain experimental observations even when there is little corroborating evidence, or indeed, when there is contravening evidence. In this case, it appears to be untenable that compensation can be at work to the necessary degree as discussed in the above references.

The discrepancy between theory and experiment is particularly glaring for heavily doped semiconductors, and this regime is the focus of the present work. On the other hand, the description of electron transport in low-doped semiconductors, for doping concentrations below $10^{16}\,\mathrm{cm}^{-3}$, is generally accurate in the sense of agreement between theory and experiment, to within about 5%–10% for the better-known semiconductors.[15–17] Nevertheless, the situation is far different for heavily doped semiconductors with dopant concentrations in the range of 10^{18}–$10^{21}\,\mathrm{cm}^{-3}$.

The objective of the present work is to achieve an agreement within a few percent in the comparison between theory and experiment for heavily doped semiconductors. For this purpose, the widely adopted Brooks–Herring theory[3,18] of electron scattering by ionized impurities is re-examined and modified.

II. IONIZED IMPURITY SCATTERING

In the following, a modification of the Brooks–Herring theory of electron scattering by ionized impurities is developed by means of the *strength* of ionized impurity scattering, and not by means of impurity screening nor by the potential energy function, which approaches have been examined by previous workers using matrix element and density functional theory methods.[1–8] Furthermore, the present treatment has nothing to do with multiply-ionized

donors per se. Neither is the discussion to be thought of as describing "dopant clusters." Instead, it is recognized fundamentally that statistically speaking in the normal course of doping, some donors will be found to reside so closely spaced with respect to one another that they may be regarded as a single electron scattering center with an effective charge of two or more fundamental charges due to constructive interference of their partial scattering waves. It is important to make clear at the outset the distinction between scattering by multiply-ionized donors and donor clusters, and scattering by *multi-ion* effects due to the proximity of donors, the latter being called *multi-ion* scattering. The former is not considered here.

Consequently, the discussion is especially concerned with heavily doped semiconductors with donor concentrations N_d in the range 10^{18}–10^{21} cm^{-3} and, hence, with typical donor spacings from 1.0 to 10 nm. But, the present theoretical treatment is not limited to degenerate conditions only; both degenerate and non-degenerate conditions are allowed. In fact, a highlight of the present result is the smooth transition from low-doped to heavily doped semiconductors.

The expression for the electron scattering rate resulting from the Brooks–Herring treatment of ionized impurity scattering due to *isolated* singly ionized impurities is[15,18]

$$\nu_{ii} = (e^4 N m d/8\pi K_s^2 \epsilon_o^2 \hbar^3 k^3)[D\ln(1+4k^2/\beta^2) - B], \tag{1}$$

where e is the fundamental charge, N is the concentration of electron scattering centers, m is the fundamental electron mass, d accounts for conduction band non-parabolicity (see below), K_s is the static dielectric constant, ϵ_o is the free-space permittivity, $k = 2\pi/\lambda$ is the conduction electron momentum divided by $\hbar$, λ is the electron de Broglie wavelength, and β is the reciprocal of the ionized impurity screening length. In particular, for Brooks–Herring scattering,

$$N = N_d^+ + N_a = n + 2N_a, \tag{2}$$

where N_d^+ and N_a are the concentrations of ionized donors and acceptors (the latter of which are taken to be fully ionized), and[15]

$$\beta^2 = (e^2/K_s\epsilon_o\kappa T)\left[\int (k/\pi)^2 f(1-f)dk + (N_d - N_a - n)(n+N_a)/N_d\right], \tag{3}$$

where f is the Fermi–Dirac distribution function and N_d is the total donor concentration, including both neutral and ionized donors The coefficients D and B are given by

$$D = 1 + 2(\beta c/k)^2 + 3(\beta c/k)^4/4 \tag{4}$$

and

$$B = (4k^2/\beta^2)/(1+4k^2/\beta^2) + 8(1+2k^2/\beta^2)c^2/(1+4k^2/\beta^2) + (3+6k^2/\beta^2 - 8k^4/\beta^4)c^4/(1+4k^2/\beta^2)(k^2/\beta^2). \tag{5}$$

The coefficient c gives the proportion of p-symmetry wave function admixture,

$$c^2 = \left[1 - \sqrt{1 + 2\hbar^2 k^2 (1/m^* - 1/m)/E_g}\right]/2, \tag{6}$$

where m^* is the conduction electron mass at the bottom of the conduction band where $k = 0$, i.e., the gamma point, and E_g is the fundamental energy gap. When $k = 0$, Eq. (6) shows that $c = 0$ and the wave function is comprised entirely of s-symmetry. The effect of conduction band non-parabolicity is given by the quantity d, where

$$1/d = 1 + (m/m^* - 1)/\sqrt{1 + (2\hbar^2 k^2/mE_g)(m/m^* - 1)}. \tag{7}$$

Equation (1) includes arbitrary degeneracy, conduction band non-parabolicity, and wave function admixture. It results from the assumption of isolated, independent scattering centers in the sense that partial waves scattered from adjacent impurities are assumed to average to zero in the summation of the matrix element for electron scattering. This is the so-called *incoherent scattering* limit. Numerical results reported below rely on a modification of Eq. (1) and iterative solutions of the Boltzmann equation for the electron Hall mobility for finite magnetic field B without further approximation. Lattice scattering is also included in the calculations, comprising piezoelectric mode scattering, acoustic mode deformation potential scattering, and inelastic polar phonon scattering, all without approximation. Details relating to the non-parabolic band structure and computational matters are set out in Appendix A.

In the present work, N of Eq. (1) will be modified as discussed in Sec. V. For present purposes, the quantity N is called the *strength* of the ionized impurity scattering process. For dilute impurities (low doping) in general, N is equal to the sum of ionized donors, ionized acceptors, and holes. For this work, N is set equal to the sum of ionized donors and acceptors, holes being absent by assumption due to the large energy gaps involved. In the present work, donors and acceptors are assumed to be singly ionized. Thus, the conduction electron concentration n equals the ionized donor concentration minus the ionized acceptor concentration. However, a new expression for the strength N must be developed for heavy doping conditions, heavy in the sense that it is no longer allowable to assume incoherent scattering.

Thus, the present objective is to examine how the strength N needs to be modified to treat closely spaced donors in heavily doped semiconductors. It has been found that multiple scattering due to closely spaced donors causes the strength N to be greater than in the Brooks–Herring case. This is a desirable outcome because experiments indicate that the electron mobility is reduced and the electron scattering rate is enhanced in heavily doped semiconductors in comparison to the Brooks–Herring theory, which is the basis of Eq. (1).

III. MULTIPLE SCATTERING

When two donors are sufficiently closely spaced, as measured in terms of the conduction electron de Broglie wavelength λ, they act to some extent as one doubly ionized scattering center, and so

on, for triply ionized centers, *ad infinitum*. These will be called *multi-ion effects,* as opposed to isolated singly ionized donors (or, single donors) and the phenomenon leads to what is called *multiple scattering* of conduction electrons. An important point to notice is that the scattering rate is proportional to the *square* of the charge on the scattering center. Singlet, doublet, and triplet donors have relative strengths of unity, four, nine, and so on. Therefore, the overall scattering rate is increased in comparison to single donors, as suggested by experiment.

For the degenerate doping range 10^{19}–$10^{22}\,\mathrm{cm}^{-3}$, typical values for the electron de Broglie wavelength λ range from 1 to 10 nm. These values are comparable to the corresponding typical donor spacings 0.5–5 nm, and this situation raises the question as to whether or not the proximity of donors might affect the electron scattering rate.

To proceed further, it is necessary to define more precisely what is meant by "closely spaced" when reference is made to multi-ion effects. Surely, one would agree that donors lying within $\lambda/20$ of one another qualify since their partial waves due to scattering would interfere with a phase difference within, at most, $2\pi/10$ radians and, on average, considerably less. That is to say, the donors scatter *coherently* within the small volume $(\lambda/20)$.[3] On the other hand, if the spacing is as much as λ itself, the partial waves would most likely average to nearly zero, which is the underlying assumption of the Brooks-Herring treatment, i.e., the donors are assumed to scatter *incoherently*. The maximum phase shift over a spacing of $\lambda/2$ would lead to constructive interference, but when averaged over a random set of such waves it leads to a somewhat smaller effect. Hence, it seems likely that the critical spacing for multiple scattering should fall within the range of λ to $\lambda/4$, but comparison to experimental results on electron mobility or further theoretical work is necessary in order to develop further refinements. For the remainder of this work it is assumed that the $\lambda/2$ dimension prevails.

IV. SPATIAL DONOR STATISTICS

The binding energy associated with covalent electron bonds in semiconductors is in the range of 1.5–3.0 eV (2.2 eV per bond for GaAs). It is so much larger than the thermal energy associated with crystal synthesis (0.05–0.15 eV) that it is likely the donor impurities arrive at the semiconductor growth interface and are bound into place without significant further lateral movement with a spatial Poisson probability distribution, although exceptions certainly are known.[19] Therefore, the donors may be assumed to be spatially Poisson distributed, and the strength factor N can be calculated on the basis of this assumption. A more-detailed discussion of this matter is set out in Appendix B.

The Poisson probability distribution function $f(i,m)$ normalized to unity is

$$f(i,\,m) = m^i/i!e^m. \tag{8}$$

The mean is m and the sample size is i. The mean is a positive real number, and the sample size is a non-negative integer. For example, if the average number of donors residing within a particular small volume is 2.8, then the probability that there will be four donors in a randomly chosen volume from a large number of identical volumes is

$$f(4,\,2.8) = \frac{2.8^4}{4!e^{2.8}} = 0.156. \tag{9}$$

So, there is about a 15% chance that will happen. The general Eq. (8) will be used below to describe the scattering strength.

V. ELECTRON SCATTERING STRENGTH

First, consider a small volume such that the mean number of ionized donors contained therein is unity so that in Eq. (8) $m = 1$. In this case, the small volume is simply equal to the reciprocal of the ionized donor concentration, or $1/(n + N_a)$, and the average donor spacing is the cube root of that. The strength parameter N for electron scattering must take into account isolated singly ionized donors, donor doublets, donor triplets, and so on, in an infinite series according to the Poisson distribution of the donor impurities. These singlet, doublet, triplet donors, etc. are taken to have charges unity, two, three, and so on.

For a total ionized donor concentration $(n + N_a)$, the effective concentration N of scattering centers, the so-called *strength* N in Eq. (1) for the electron scattering rate ν_{ii}, can be expressed as follows under the assumption of the Poisson distribution,

$$N = (n + N_a)\left(1 - \frac{2}{2!e} - \frac{3}{3!e} - \frac{4}{4!e} - \dots\right) + (n + N_a)\left(\frac{2^2}{2!e} + \frac{3^2}{3!e} + \frac{4^2}{4!e} + \dots\right) + N_a. \tag{10}$$

The first term comprises the usual ionized donor concentration $(n + N_a)$ with appropriate weighted reductions for donors otherwise assigned to multiple scattering, i.e., factor 2 for doublet donors, three for triplet donors, and so on. The second term provides for scattering by multi-ion donors, with squared charge weightings of 4, 9, 16, etc. Acceptors, represented by N_a are incorporated in unmodified form as simply N_a in Eq. (10) because they are present, if at all, in small concentrations when the donor concentration is large as will be shown below. Equation (10) can be reduced to

$$N/(n + N_a) = 1 + \sum_0^\infty \frac{i(i-1)}{i!e} + N_a/(n + N_a). \tag{11}$$

But this is simply related to the series (see Appendix C),

$$\sum_0^\infty i^2/i! = 2e \tag{12}$$

and

$$\sum_0^\infty i/i! = e. \tag{13}$$

So,

$$N = 2(n + N_a) + N_a = 2N_d^+ + N_a. \tag{14}$$

In this case, Eq. (14) shows that the scattering strength due to ionized donors is enhanced by a factor of two in comparison to Brooks–Herring scattering because of multiple scattering; compare Eqs. (2) and (14). Thus, if the mean number of donors contained in the small volume over which coherent scattering occurs is unity, the scattering strength is enhanced by a factor of two, and the electron mobility is decreased by a factor of two. This agrees only roughly with experiment, which indicates a factor of about 1.4–1.8. Clearly, the mean number of donors cannot be quite as large as unity, i.e., the small volume cannot be so large as $1/(n+N_a)$. Nevertheless, it is remarkable that the simple assumption $m=1$ gives a result lying within about 40% of the value needed in order to agree with experiment.

More generally, allowing for an arbitrary mean number m of donors contained within the coherent scattering volume, the scattering strength is

$$N=(n+N_a)\left(1-\frac{2m^2}{2!e^m}-\frac{3m^3}{3!e^m}-\frac{4m^4}{4!e^m}-\ldots\right)+(n+N_a)\left(\frac{2^2m^2}{2!e^m}+\frac{3^2m^3}{3!e^m}+\frac{4^2m^4}{4!e^m}+\ldots\right)+N_a. \quad (15)$$

Or,

$$N/(n+N_a)=1+\sum_0^\infty \frac{i(i-1)m^i}{i!e^m}+N_a/(n+N_a). \quad (16)$$

This result can be expressed as (see Appendix C)

$$N/(n+N_a)=1+m^2+N_a/(n+N_a). \quad (17)$$

Equation (17) shows that if the mean number of donors lying within a small volume corresponding to coherent scattering is taken to be $m=0.63$ or 0.78, the scattering strength is enhanced by a factor of 1.4 or 1.6, in fair agreement with the experiment. A more thorough analysis is given in the next section.

VI. ELECTRON SCATTERING RATE INCLUDING MULTIPLE SCATTERING

The improved agreement with experiment dependent on the expected size of the volume over which coherent multiple scattering occurs indicates that the assumption concerning closely spaced ionized donor scattering is, in fact, a plausible explanation of the experimental results. Nevertheless, the question naturally arises as to the precise dimensions of the small coherent scattering volume in comparison to the electron wavelength, whose linear dimensions are assumed to be $\lambda/2$, as discussed above. A proper quantum mechanical description of the problem along the lines first set out by Meyer and Bartoli[6,7] would be highly desirable.

Under the assumption that the linear dimension of the coherent scattering volume is $\lambda/2$, the scattering strength in Eq. (1) becomes, from Eq. (17),

$$N=(n+N_a)[1+(n+N_a)^2(\pi/k)^6]+N_a. \quad (18)$$

This expression replaces the quantity N in Eq. (1). Thus, by comparison to Eq. (2), it can be seen that the electron scattering rate is enhanced over the Brooks-Herring rate, especially at larger doping concentrations, and because of the sixth power dependence on k, the onset of multi-ion scattering is rather abrupt. The calculated onset of multi-ion enhancement depends on the conduction electron effective mass m^* but it occurs for donor concentrations above 6×10^{17} and $7\times10^{18}\,\mathrm{cm}^{-3}$ for $m^*=0.066$ and 0.318 m, appropriate to GaAs and ZnO.

VII. RESULTS

Material parameters used in the theoretical calculations below are listed in Table I. These are, for the most part, the same as those given earlier[15] except for four revisions relating to ZnO and to GaN.[20] Also, it is shown below that the acoustic deformation potential E_{ac} for ZnO must be revised upward from 3.8 eV given earlier[15] to 7.4 eV in the present work.

TABLE I. Material parameters at 300 K.

Material	GaAs	ZnO	GaN	Sn	Units
Static dielectric constant, K_s	12.91	8.12	10.19	24.0	…
Optical dielectric constant, K_∞	10.91	3.72	5.35	…	…
Optical phonon temperature, T_{po}	419	837	1056	…	K
Longitudinal elastic constant, c_l	140	207	372	82.1	GPa
Acoustic deformation potential, E_{ac}	8.6	7.4	8.4	3.2	eV
Piezoelectric coefficient, P_{pe}	0.052	0.21	0.145	…	…
Kane energy gap,[a] E_g	1.48	3.43	3.39	0.413	eV
Spin–orbit splitting, Δ	…	…	…	0.70	eV
Conduction electron mass,[b] m^*/m	0.066	0.318	0.22	0.0236	…

[a]Energy gap used in Kane's band theory, determinative of conduction band non-parabolicity, which is slightly greater than the energy gap E_g measured by optical absorption, for instance. Use of the Kane E_g vs the optical E_g has minimal effect on calculated mobility values, the result usually differing by less than 0.2%.

[b]The electron effective mass m^* is adjusted for polaron effects.

A. GaAs

Due to intense commercial development of electronic and optoelectronic devices based on the semiconductor GaAs, a vast amount of electron Hall mobility data are available for a wide range of doping conditions.[9–17] Room-temperature experimental results (nominally for $T = 300$ K) are shown in Fig. 1.[9,11,21–23] Comparisons between theory and experiment are shown for the present treatment of multiple scattering by the solid curve (*green*), which is compared to the Brooks–Herring theory shown as the dashed curve (*red*).

The small disagreement between theory and experiment in Fig. 1 near 10^{15} cm^{-3} is insignificant, merely depending on low-level unintentional impurities (termed *background doping*). The acceptor concentration is set equal to $N_a = 3 \times 10^{15}$ cm^{-3} for the solid curve and to 2×10^{15} cm^{-3} for the dashed-dotted curve (*blue*), which shows the small effect of compensation in the low-doped region.

Present concern is with the heavily doped range above 10^{17} cm^{-3} where one can easily see that the multiple scattering theory is a significant improvement over the Brooks–Herring theory, in comparison with experimental results. Clearly, the solid theoretical curve, because it assumes very little dopant compensation, should give an upper bound for the electron Hall mobility and this is seen to be the case within a few percent in Fig. 1.

It is notable that data on bulk GaAs (open and solid squares[11]) grown at 1238 °C in silica crucibles exhibit substantially lower mobility values for reduced doping levels. By way of explanation, contamination from the silica crucible is expected, as well as background doping by carbon acceptors at the level of mid-10^{15} to mid-10^{16} cm^{-3}. Nevertheless, somewhat above 10^{17} cm^{-3}, the data for bulk GaAs fall nicely into line with results for epitaxial GaAs.[9,21–23]

B. ZnO

ZnO is an interesting wide-bandgap semiconductor in the sense that it possesses a very large direct conduction band energy range, free from complications due to higher-lying indirect conduction bands.[24] The Γ minimum prevails in the conduction band from the Γ minimum to the A minima separated by (5.9–3.4) = 2.5 eV. This bodes well for high levels of electrical conductivity, even at elevated temperatures. In comparison, this quantity for GaAs is merely 0.3 eV and GaAs exhibits a transition to electron conduction in the indirect L minima beginning at a temperature of 600 K.[15] The indirect minima lead to reduced electron mobility due to intervalley scattering. This situation needs to be avoided if high electrical conductivity is to be achieved.

Figure 2 gives Hall measurement results for a laser-ablated Ga-doped ZnO sample of thickness 575.5 nm with a measured[25] conduction electron concentration $n = 8.84 \times 10^{20}$ cm^{-3}. The comparison between theory and experiment is for the present multiple scattering treatment (*green curve*) and the Brooks–Herring theory (*red curve*), as indicated in the figure, assuming no acceptor compensation. The agreement for the former is within 1%, while for the Brooks–Herring case, theory and experiment disagree by 80%–100%. In the former case, there is a rather small trend toward disagreement at the highest temperatures (see Fig. 3), and this

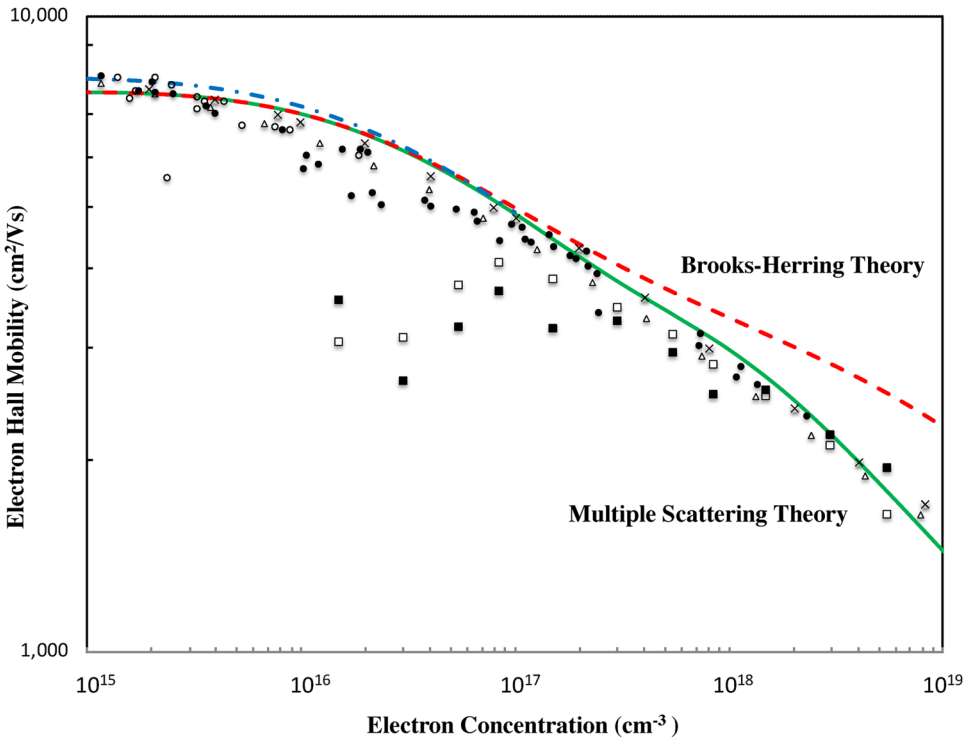

FIG. 1. Room-temperature (300 K) electron Hall mobility of n-type GaAs. The experimental data points use a variety of magnetic field strengths, ranging from a few hundred Gauss to 10 kG.[9,11,21–23] The theoretical curves are iterative solutions of the Boltzmann equation for electron Hall mobility with magnetic field $B = 10$ kG and include arbitrary degeneracy, wave function admixture, and conduction band nonparabolicity. The curves assume acceptors as noted in the text.

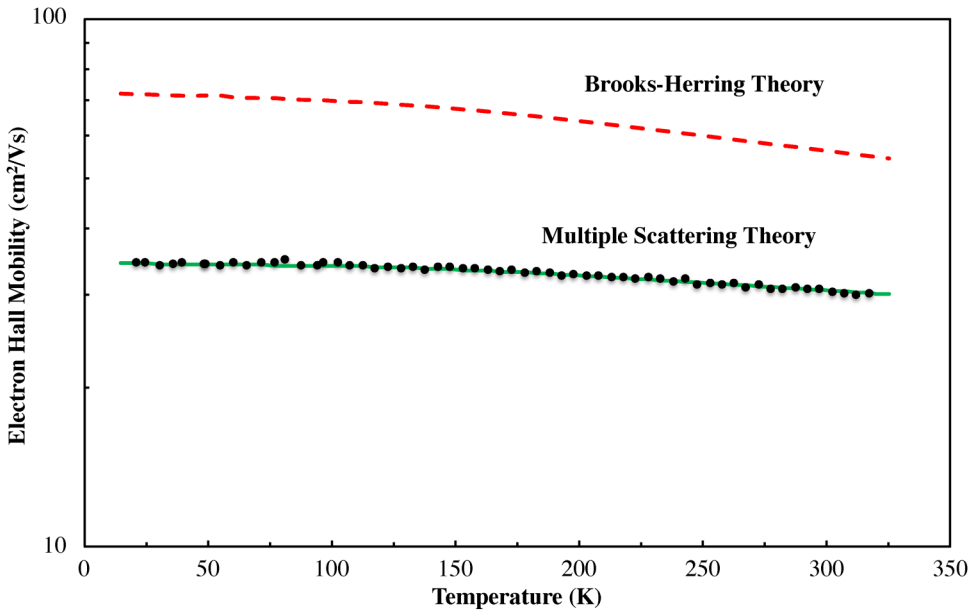

FIG. 2. Temperature-dependent electron Hall mobility of heavily Ga-doped ZnO with n = 8.84 × 10^{20} cm^{-3}. The ZnO layer was synthesized by pulsed-laser deposition. The experimental data points use a 10 kG magnetic field.[25] The curves are theoretical for the two cases shown.

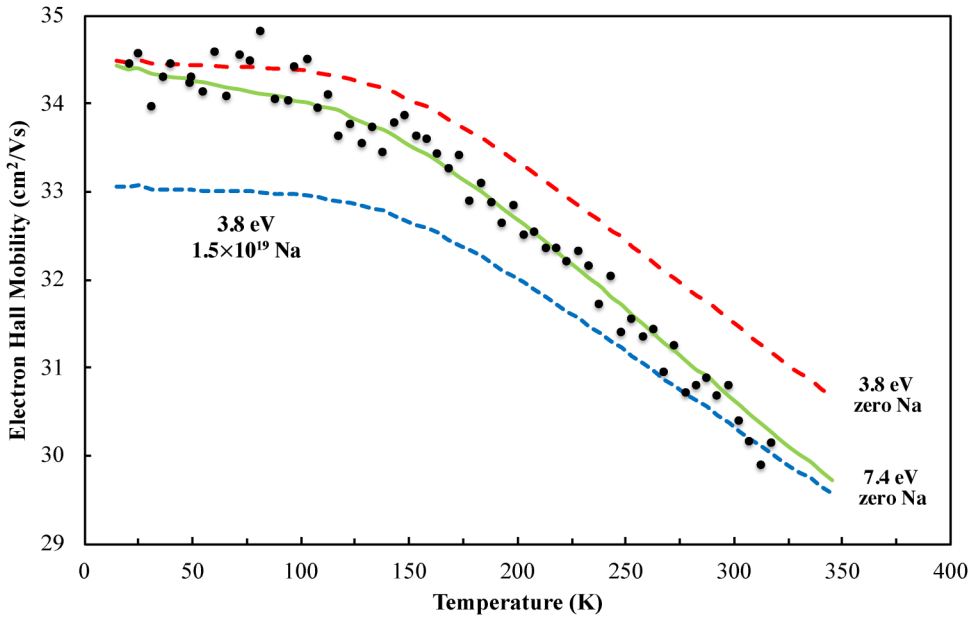

FIG. 3. Temperature-dependent electron Hall mobility of heavily Ga-doped ZnO on an expanded scale. When E_{ac} = 3.8 eV, acceptor compensation alone does not give agreement between theory and experiment. Alternatively, when E_{ac} = 7.4 eV is used, no acceptor compensation is necessary.

behavior might be assignable to indirect band conduction or deep donors, but the precise cause is unknown at this time. Certainly, the agreement between experiment and multiple scattering theory is well-within the desired 5%–10% range set out in Sec. I and is a testament to the high quality of the experimental work.

The theoretical curves are iterative solutions of the Boltzmann equation including degeneracy, non-parabolic conduction band, and wave function admixture. The solid curve includes the present multiple scattering theory while the dashed curve is based on the Brooks-Herring theory, assuming no acceptors in both cases. Agreement between theory and experiment in the former case is within 1% (one standard deviation).

Figure 3 shows the same results on an expanded scale in order to examine two questions regarding the acoustic deformation potential E_{ac} and compensating acceptors. The solid curve (*green*) is the same as in Fig. 2; it uses $E_{ac} = 7.4$ eV and no acceptors. The dashed curve (*red*) uses $E_{ac} = 3.8$ eV and no acceptors. The dotted curve (*blue*) uses $E_{ac} = 3.8$ eV and 1.5×10^{19} cm^{-3} acceptors. Clearly, acceptor compensation alone (dotted curve) does not provide the correct temperature dependence when the original[15] $E_{ac} = 3.8$ eV value is used. On the other hand, for $E_{ac} = 7.4$ eV and no acceptor compensation, the agreement between theory and experiment is quite satisfactory. Thus, it appears that acceptor compensation for this heavily doped ZnO sample is not called for.

In Fig. 4, results are shown for another heavily Ga-doped ZnO sample.[26] In this case, the measured conduction electron concentration is $n = 1.108 \times 10^{21}$ cm^{-3} and the sample thickness is given as 278 nm.[26] Comparison is made between the Brooks–Herring theory (*red dashed curve*) and the multi-ion theory (*green solid curve*). The middle curve (*blue dotted curve*) assuming a compensating acceptor concentration of 2.0×10^{20} cm^{-3} shows that it would likely require a very large amount of compensation to force agreement with the Brooks-Herring theory, amounting to 41% of the donor concentration.

The lower curve for the multi-ion theory assumes a compensating acceptor concentration of 6.0×10^{18} cm^{-3}, which amounts to merely 0.53% of the donor concentration, an amount so small as to fall within the uncertainty of both the theory and the experiment, as discussed in more detail below.

The results of Fig. 4 are repeated in Fig. 5 on an expanded scale, in order to show the effect on the calculated mobility of varying the acoustic deformation potential from 3.8 (*red curve*) to 7.4 eV (*green curve*). The ZnO sample of Fig. 3 also uses 7.4 eV, and this appears from the figure to be the preferred value for ZnO, as listed in Table I.

Although the multi-ion theory (*green curve*) agrees with the experiment within 0.26% (one standard deviation), this must be regarded as fortuitous and not physically significant for the following reasons. First, the sample thickness is given as 278 nm, but it seems doubtful this could be known with accuracy much better than 1%, especially when one is concerned with the electrically active thickness and not merely the metallurgical thickness, i.e., dopant nonuniformities and interface depletion need to be considered. Second, interface scattering may be important for such a thin sample; this effect is estimated in this case to reduce the mobility by 0.96%. Consequently, not much significance should be attached to comparisons more precise than that.

It may be that there is actually very little acceptor compensation in this ZnO sample. Figure 6 shows the experimental data from Fig. 5 compared to the multi-ion theory assuming no acceptor

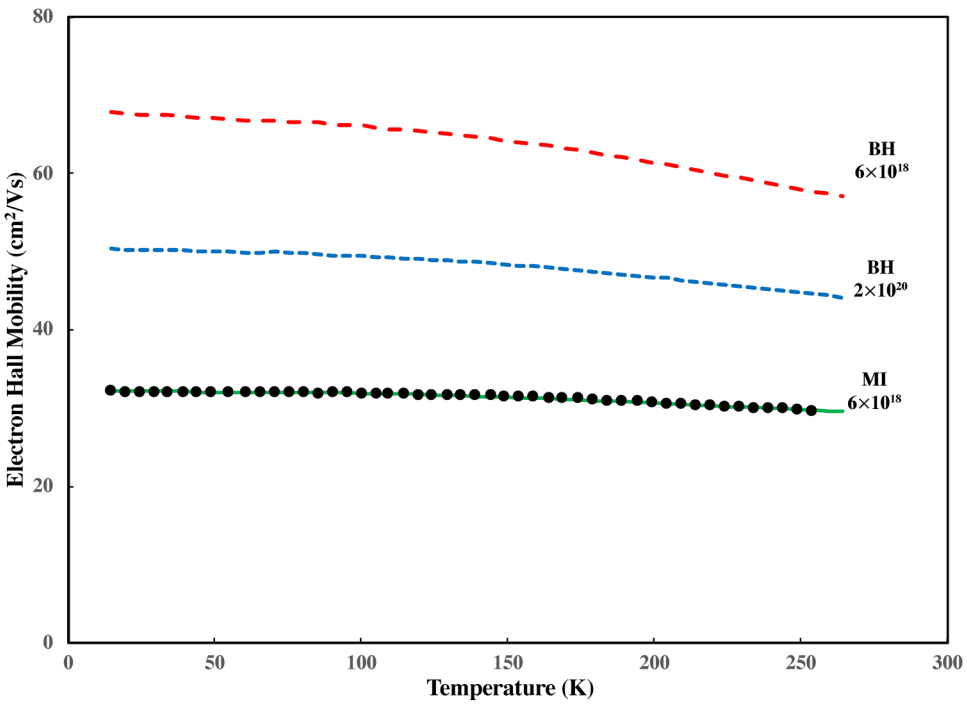

FIG. 4. Temperature-dependent electron Hall mobility of heavily Ga-doped ZnO with $n = 1.108 \times 10^{21}$ cm^{-3} conduction electron concentration.[26] Agreement between multi-ion theory (lower curve) and experiment is within 1%. Explanation by means of compensating acceptors (center curve) would require a rather large acceptor concentration, as suggested by the curve labeled 2×10^{20}, which is calculated for $N_a = 2.0 \times 10^{20}$ cm^{-3}.

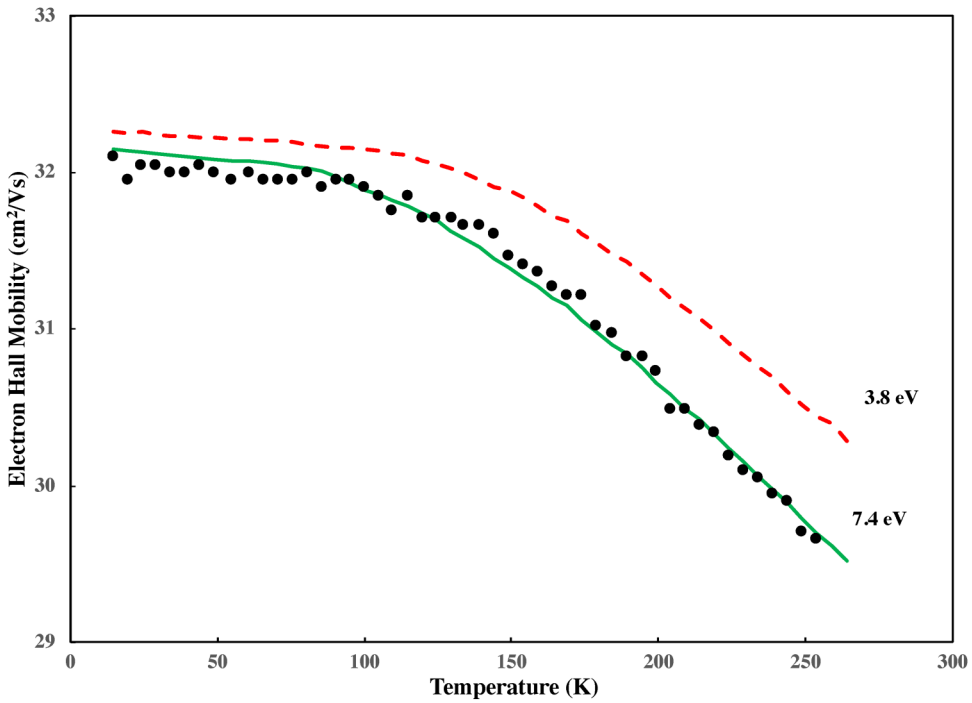

FIG. 5. Temperature-dependent electron Hall mobility of heavily Ga-doped ZnO.[26] Agreement between theory and experiment is 0.26% (one standard deviation).

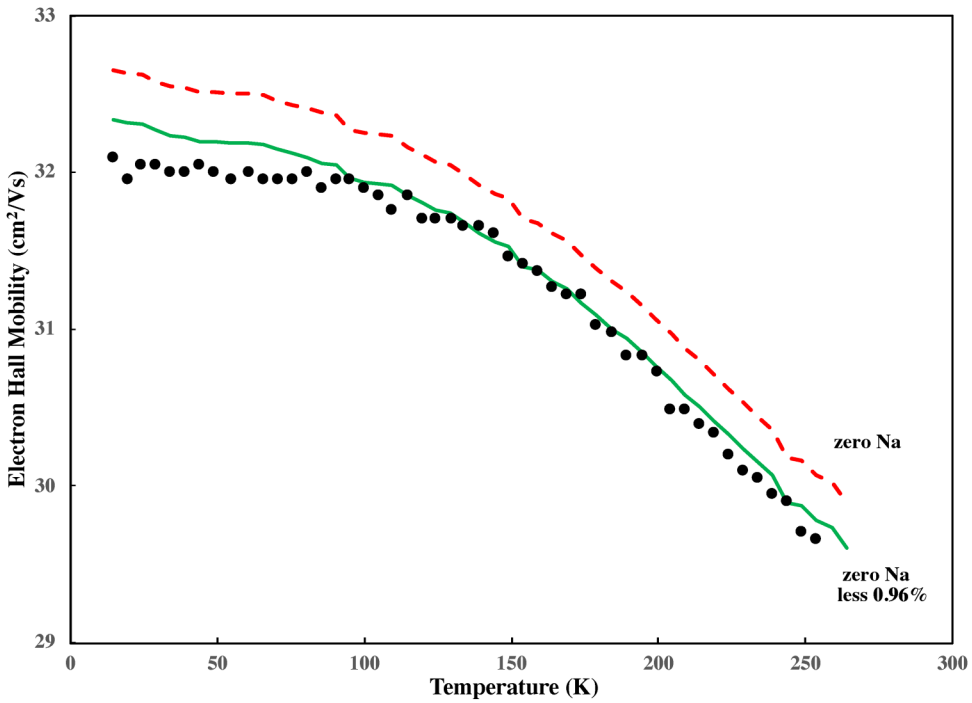

FIG. 6. Electron Hall mobility showing the effect of interface scattering on Hall mobility. Both curves assume zero acceptor compensation.

compensation at all, both with (*green curve*) and without (*red curve*) an interface scattering correction of 0.96%. The solid curve for the multi-ion theory agrees with the experiment within 0.3% (one standard deviation) overall and at worst, within 1.1% at the lowest temperatures.

C. GaN

Theoretical results and experimental data for room-temperature GaN are plotted in Fig. 7. It has proven difficult in many cases to obtain experimental data which are free from the effects of material nonuniformities, accumulation layers at interfaces,[31] threading dislocations,[32] and shunt conduction paths. This behavior becomes evident when low-temperature freeze-out fails before freeze-out has occurred over a range smaller than two or three orders of magnitude. Exceptional efforts have been made in this regard, such as measurements on free-standing layers of GaN[31,33] and the use of p-type isolation structures between the substrate and the epitaxial layer.[32]

The wide data scatter in Fig. 7, especially for the lower doping range, is probably symptomatic of these types of nonuniformity problems. Nevertheless, the highest data suggest that the correct material parameters are being used to generate the theoretical curves. Much of the data fall well-below the theoretical curves, perhaps due to experimental difficulties associated with nonuniformities, but when exceptional efforts[27,32] are made, it is possible to get results that are more comparable to the theory, as shown, especially by the solid circles even at electron concentrations in the neighborhood of $3 \times 10^{16}\,\mathrm{cm}^{-3}$.

Obviously, the multiple scattering theory excels over the Brooks–Herring theory for heavy doping, which is shown clearly in Fig. 7. The good agreement with multiple scattering theory for doping levels in the 2×10^{19}–$2 \times 10^{20}\,\mathrm{cm}^{-3}$ range is especially gratifying.

D. α-Sn

Of course, there is nothing that inherently limits the present multiple scattering theory to wide-bandgap semiconductors; it should be equally applicable to zero-gap semimetals as well, provided proper account is taken of the wave functions for conduction electrons.[34] The semimetal α-Sn is a case in point, the data of which indeed show that the Brooks-Herring theory lies noticeably above the experimental results. Table II shows two results comparing theory and experiment.[15,35–38] In the table, the notations MS and BH represent multiple scattering and Brooks-Herring. The two right-hand columns show that the Brooks–Herring theory lies 33%–49% above the experiment, whereas the multiple scattering results lie 8%–13% above experiment; perhaps a not very convincing improvement, but an improvement nevertheless. It is unclear how much of the discrepancy is due to the theory and how much is due to the experiment, so little more can be said.

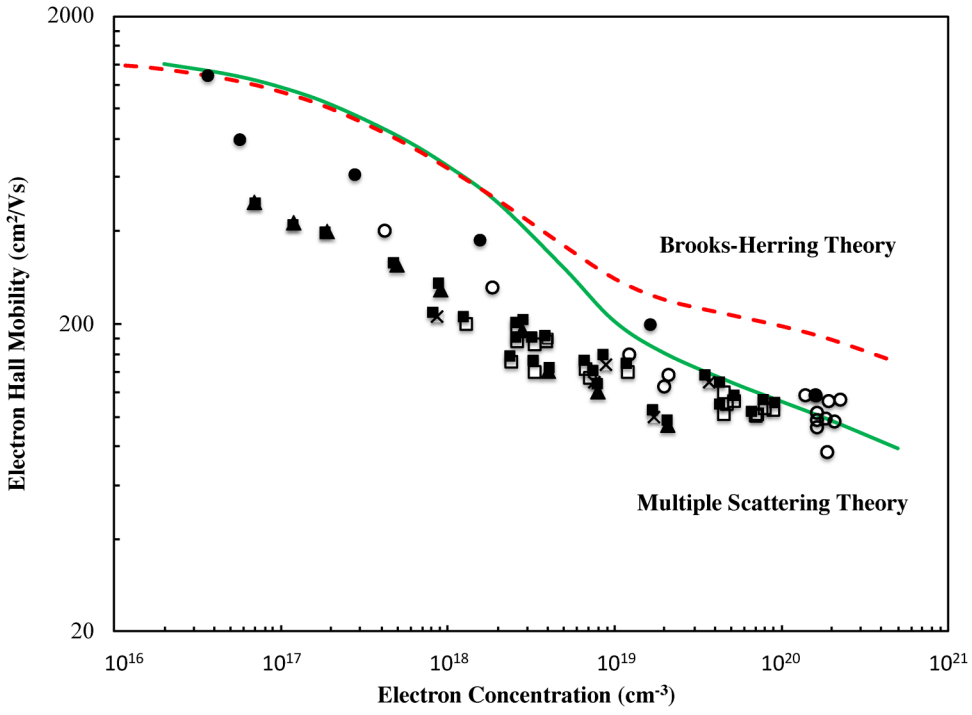

FIG. 7. Electron Hall mobility of doped GaN. The solid curve includes the present multiple scattering (*green curve*), while the dashed curve relies on the Brooks–Herring theory (*red curve*). Experimental data are given by data points.[27–30].

TABLE II. Electron Hall mobility of α-Sn, T = 4.2 K.

Experiment[15] n (cm^{-3})	Experiment[15] 1 kG mobility	MS theory Hall mobility	BH theory Hall mobility	MS/experiment Ratio	BH/experiment Ratio
5.06×10^{16}	118 072	133 900	176 318	1.13	1.49
4.80×10^{17}	62 876	67 090	83 729	1.08	1.33

VIII. CONCLUSION

Notwithstanding that the present approach to the multiple scattering problem does not rely on a development from the matrix-element level as has been carried out by previous workers,[1–3,6–8] nor by the novel molecular dynamics approach introduced by Joshi and Ferry,[39] the present scheme which relies on a modification of the *strength* term for ionized impurity scattering appears to be moderately successful. It has the further advantage that, under the assumption of the dimension for coherent scattering being equal to one-half the conduction electron de Broglie wavelength, there are no adjustable parameters. Indeed, the strong dependence (sixth power) on electron momentum k shown in Eq. (18) ensures that the half-wavelength assumption must be quite nearly correct, for if the coherent dimension were to be reduced by even as little as 10%, the correction to Brooks–Herring scattering would be reduced by nearly 50%, which would clearly not agree with the experimental data. Also impressive is the fact that large energy-gap, medium energy-gap, and zero energy-gap materials can be at least tentatively explained.

ACKNOWLEDGMENTS

The authors have benefited greatly from the generosity of the following who shared thoughts and data relating to the multiple scattering problem, namely, J. S. Speck (University of California-Santa Barbara), H. Morkoç (Virginia Commonwealth University), J. R. Meyer (Naval Research Laboratory), D. C. Look (Wright State University), K. D. Leedy (Air Force Research Laboratory), E. C. H. Kyle (University of California-Santa Barbara), D. K. Gaskill (Naval Research Laboratory), and David L. Cronin (Washington University). This research was supported by the Air Force Office of Scientific Research (Project No. FA9550-23RXCOR022).

AUTHOR DECLARATIONS

Conflict of Interest

The authors have no conflicts to disclose.

Author Contributions

D. L. Rode: Writing – original draft (lead). **John S. Cetnar:** Writing – review & editing (supporting).

APPENDIX A: BAND STRUCTURE AND COMPUTATION

Pertaining to details of the band structure and computational methodology, the non-parabolic band theory of Kane is used assuming negligible spin–orbit splitting.[40–42] The conduction electrons have admixed wave functions,

$$\varphi_{c\alpha} = a[iS\downarrow]' + c[Z\downarrow]', \tag{A1}$$

where the subscript c denotes wave function admixture and α is the spin index. The a and c coefficients are normalized to unity,

$$a^2 + c^2 = 1. \tag{A2}$$

The quantity c is given by Eq. (6). The non-parabolic conduction band energy-vs-momentum relation is given simply in terms of the two fundamental material parameters, energy gap E_g and conduction electron mass m^*,

$$E = \hbar^2 k^2/2m + (E_g/2)\left[\sqrt{1 + 2\hbar^2 k^2 (m/m^* - 1)/mE_g} - 1\right]. \tag{A3}$$

Notice that $E = 0$ when $k = 0$ at the gamma point, i.e., the minimum of the conduction band. But, the energy is sub-parabolic to a greater and greater extent as the momentum k increases causing the electron "effective mass" to increase over the value m^*, which is called the conduction electron mass.

The numerical solution of the Boltzmann equation relies on the iterative solution of the finite difference equation, which results from the inelastic nature of electron scattering by optical phonon modes.[42] The sequence of iterations typically comprises four to seven iterations to achieve better than 0.1% convergence. The finite difference equation is cast in the form of a contraction mapping,[43] ensuring: (i) existence of the solution, (ii) uniqueness of the solution, and (iii) exponential convergence to the solution. Therefore, any fluctuating residuals which are noticed in the iteration sequence can be ascribed to the small but finite momentum increments used to implement the solution of the finite difference equation. For this reason, and in order to achieve computational accuracy generally within 0.1%, the momentum range is divided into 400 000 equal increments extending from $k = 0$ to 13 κT above the greater of the gamma point or the Fermi level, where the Fermi–Dirac function will have declined to values smaller than 0.001%. This degree of rigor, which at first may seem excessive, is actually found to be necessary for the extremely high levels of degeneracy encountered in this work where the Fermi level may be as large as one-thousand times the thermal energy κT.

On rare occasions, obvious fluctuations amounting to as much as 0.4% of the calculated electron Hall mobility are noticed, but these are easily perceived and removed numerically. They are thought to be due to numerical underflow in the Fortran computer program. To confirm the accuracy of the Fermi level calculations in the limit of high degeneracy, recourse can be had to the analytical

expression given by Cetnar and Rode[44] for the Fermi level, even in the presence of non-parabolic bands,

$$E_F = E_o - (E_g/2)\left[1 - \sqrt{4E_o(m/m^* - 1)/E_G}\right], \quad \text{(A4)}$$

where

$$E_o = \hbar^2 k_F^2/2m \quad \text{(A5)}$$

For example, given $n = 1.108 \times 10^{21}\ cm^{-3}$ and $T = 14.4$ K (*apropos* the ZnO sample of Fig. 4) the Fortran computer program gives the Fermi Level as $E_F = 1.086\,50$ eV, while the Cetnar–Rode analytical equation gives $E_F = 1.086\,55$ eV in substantially perfect agreement.

APPENDIX B: DONOR SPATIAL DISTRIBUTION

Regarding the motion of dopants by migration laterally along the growing interface, DiLorenzo[22] finds an activation energy of 5.5 eV for Si dopant incorporation into GaAs by vapor-phase epitaxial crystal growth, which we suggest is likely nearly equal to the chemical binding energy of the dopant on the growing interface since the covalent bonds in bulk GaAs possess energy of 2.2 eV per bond and on the growing interface there will be two or three covalent bonds (4.4–6.6 eV) for chemisorbed dopants, corresponding to the tetrahedral bonding scheme of GaAs. Consequently, significant lateral dopant migration along the growing crystal interface hardly seems significant, according to the reasoning set out below.

The spatial distribution of dopants arriving at the growing interface of the crystal, whether by means of a vapor phase or a liquid phase are not subject to any known organizing principle, except perhaps, electrostatic Coulomb repulsion or attraction. But Coulomb effects can be shown to be negligible for the conditions considered in this work, where the atomic concentrations of dopant species are much smaller than the atomic concentrations of the crystals themselves (see below). Therefore, the spatial distribution of dopants arriving at the growing interface will be random in the sense of yielding a Poisson spatial distribution. On the growing interface, the dopants may be weakly physisorbed where, again, they may migrate randomly. However, once the dopants are incorporated into covalent bonds (i.e., chemisorbed), they will no longer migrate to any significant degree, as the following argument shows.

It can be shown that Coulomb effects may be disregarded as follows. The atomic ionization energy E_1 of possible dopant species is generally in the range of 8–11 eV. For example, relevant to the doping of GaAs and GaN, atomic Si with $E_1 = 8.2$ eV gives the probability of being ionized at a growth temperature of 1000 K as $e^{-8.2 \times 11\,604/1\,000} = 4.74 \times 10^{-42}$, which is so negligibly small that it may be presumed that the dopant species are electrostatically neutral prior to their incorporation into the crystal. In view of the miniscule probability factor, it is unlikely that consideration of chemically radical forms of the dopant species would alter this conclusion. While the foregoing pertains to crystal growth from the vapor phase, in the case of liquid-phase crystal growth, ionized species would be screened by the surrounding liquid metal solvent and Coulomb interactions would be negligible.

Given that Coulomb effects can be disregarded, the argument may be continued as follows. A typical epitaxial crystal growth rate is about 6 μm per hour. For GaAs with its lattice parameter of 565 pm, the crystal monolayer thickness is 283 pm so the time required to deposit one monolayer is $3600 \times 283/6 \times 10^6 = 0.17$ s, after which the dopant is buried by the next monolayer and presumably immobilized. On the other hand, the attempt frequency for a dopant atom to jump from one crystal site to the next is approximately equal to the polar phonon vibration frequency, which is given for GaAs in Table I as being equivalent to a Debye temperature of $T_{po} = 419$ K. This number translates into a vibration (or attempt) frequency of $kT_{po}/\hbar = 5.49 \times 10^{13}$ per second. Therefore, in 0.17 s, there will be 9.31×10^{12} attempts. However, the probability that a dopant will surmount the potential energy barrier (5.5 eV) resisting motion into the next crystal site is related to the crystal growth temperature T_g by the exponential $e^{-5.5\ eV/Tg}$. For typical crystal growth temperatures around 1000 K, this probability is equal to $e^{-11\,604 \times 5.5/1\,000} = e^{-63.8}$ so the probability, on average, that a dopant will migrate a distance of one crystal site before being buried by the next monolayer is $9.31 \times 10^{12} \times e^{-63.8} = 1.78 \times 10^{-15}$. This is a very small number indeed, so small that it is quite justifiable to assume a Poisson spatial distribution for chemisorbed dopants without further dopant migration.

APPENDIX C: INFINITE SERIES SUMMATION

The Napierian base of logarithms e can be expressed as an infinite series for real values of x,

$$e^x = \sum_0^\infty x^i/i! \quad \text{(C1)}$$

from which it follows that,

$$\sum_1^\infty 1/i! = e - 1 \quad \text{(C2)}$$

$$\sum_1^\infty i/i! = \sum_0^\infty i/i! = e \quad \text{(C3)}$$

and,

$$\sum_1^\infty i^2/i! = \sum_0^\infty i^2/i! = 2e \quad \text{(C4)}$$

The derivation of Eq. (17) can be carried out starting from Eq. (16),

$$\sum_0^\infty i(i-1)m^i/i! = \sum_0^\infty i^2 m^i/i! - \sum_0^\infty i m^i/i! \quad \text{(C5)}$$

$$\sum_0^\infty i(i-1)m^i/i! = \sum_1^\infty i m^i/(i-1)! - \sum_1^\infty m^i/(i-1)! \quad \text{(C6)}$$

The last term is,

$$\sum_1^\infty m^i/(i-1)! = m\sum_1^\infty m^{i-1}/(i-1)! = m\sum_0^\infty m^i/i! = me^m \quad \text{(C7)}$$

The second-last term of Eq. (C6) is,

$$\sum_1^\infty im^i/(i-1)! = m\sum_1^\infty im^{i-1}/(i-1)! \tag{C8}$$

$$\sum_1^\infty im^i/(i-1)! = m\sum_1^\infty (i-1)m^{i-1}/(i-1)! + m\sum_1^\infty m^{i-1}/(i-1)! \tag{C9}$$

$$\sum_1^\infty im^i/(i-1)! = m\sum_0^\infty im^i/i! + m\sum_0^\infty m^i/i! \tag{C10}$$

$$\sum_1^\infty im^i/(i-1)! = me^m + m^2e^m \tag{C11}$$

Therefore,

$$\sum_0^\infty i(i-1)m^i/i! = m(m+1)e^m - me^m \tag{C12}$$

$$\sum_0^\infty i(i-1)m^i/i! = m^2e^m \tag{C13}$$

These results provide the basis for Eqs. (12), (13), and (17).

DATA AVAILABILITY

The data that support the findings of this study are available within the article.

REFERENCES

[1]E. J. Moore and H. Ehrenreich, Solid State Commun. **4**, 407 (1966).
[2]E. J. Moore, Phys. Rev. **160**, 618 (1967).
[3]L. M. Falicov and M. Cuevas, Phys. Rev. **164**, 1025 (1967).
[4]D. Chattopadhyay, Philos. Mag. B **43**, 165 (1981).
[5]D. Chattopadhyay and H. J. Queisser, Rev. Mod. Phys. **53**, 745 (1981).
[6]J. R. Meyer and F. J. Bartoli, J. Phys. C Solid State Phys. **15**, 1987 (1982).
[7]J. R. Meyer and F. J. Bartoli, Phys. Rev. B **36**, 5989 (1987).
[8]K. L. Kovalenko, S. I. Kozlovskiy, N. N. Sharan, and E. F. Venger, J. Appl. Phys. **131**, 125708 (2022).
[9]E. Kuphal, A. Schlachetzki, and A. Pöcker, Appl. Phys. **17**, 63 (1978), solid circles in Fig. 1.
[10]H. Poth, H. Bruch, M. Heyen, and P. Balk, J. Appl. Phys. **49**, 285 (1978).
[11]J. B. Mullin, A. Royle, and S. Benn, J. Cryst. Growth **50**, 625 (1980), solid and open squares in Fig. 1.
[12]E. Kuphal, J. Cryst. Growth **54**, 117 (1981).
[13]E. Veuhoff, M. Maier, K.-H. Bachem, and P. Balk, J. Cryst. Growth **53**, 598 (1981).
[14]D. A. Anderson, N. Apsley, P. Davies, and P. L. Giles, J. Appl. Phys. **58**, 3059 (1985).
[15]D. L. Rode, in *Semiconductors and Semimetals*, edited by R. K. Willardson and A. C. Beer (Academic Press, New York, 1975), Vol. 10, Ch. 1.
[16]C. M. Wolfe and G. E. Stillman, Appl. Phys. Lett. **27**, 564 (1975).
[17]W. Walukiewicz, L. Lagowski, L. Jastrzebski, M. Lichtensteiger, and H. C. Gatos, J. Appl. Phys. **50**, 899 (1979).
[18]H. Brooks, Adv. Electron. Electron. Phys. **7**, 85 (1955).
[19]Dopant species Li in Ge, B in Si, and Zn in GaAs readily come to mind.
[20]D. L. Rode, AFRL Final Report, AFRL-RY-WP-TR-2021-0183, August 2021, where revisions to K_s, K_∞, and c_l for GaN and to c_l for ZnO are developed.
[21]M. R. Borzel and G. E. Stillman, *Properties of Gallium Arsenide*, EMIS Data Reviews, Series No. 16 (INSPEC, London, 1996), p. 106, x's in Fig. 1.
[22]J. V. DiLorenzo, J. Cryst. Growth **17**, 189 (1972), background Si-doped, VPE GaAs, open circles in Fig. 1.
[23]M. Sotoodeh, A. H. Khalid, and A. A. Rezazadeh, J. Appl. Phys. **87**, 2890 (2000), open triangles in Fig. 1.
[24]C. Yan, "Electronic structure and optical properties of ZnO," Ph.D. thesis (Oregon State University, 1994), Ch. 3.
[25]K. D. Leedy and J. S. Cetnar, private communication (2019).
[26]D. C. Look, K. D. Leedy, L. Vines, B. G. Svensson, A. Zubiaga, F. Tuomisto, D. R. Doutt, and L. J. Brillson, Phys. Rev. B **84**, 115202 (2011).
[27]E. C. H. Kyle and J. S. Speck, personal communication, solid circles in Fig. 7 (2022).
[28]M. N. Fireman, G. L'Heureux, F. Wu, T. Mates, E. C. Young, and J. S. Speck, J. Cryst. Growth **508**, 19 (2019), open circles in Figs. 3 and 4.
[29]H. Morkoç, *Handbook of Nitride Semiconductors and Devices* (Wiley, 2008), Vol. 1, Figs. 51 and 52, solid squares and open triangles in Fig. 7.
[30]D. L. Rode and D. K. Gaskill, J. Appl. Phys. **99**, 036106 (2006), open squares and x's in Figs. 3 and 4.
[31]M. N. Fireman, G. L'Heureux, F. Wu, T. Mates, E. C. Young, and J. S. Speck, J. Cryst. Growth **508**, 19 (2019), open circles in Fig. 7.
[32]E. C. H. Kyle, S. W. Kaun, P. G. Burke, F. Wu, Y.-R. Wu, and J. S. Speck, J. Appl. Phys. **115**, 193702 (2014), solid circles in Figs. 3 and 4.
[33]D. L. Rode and D. K. Gaskill, J. Appl. Phys. **99**, 036106 (2006), open squares and x's in Fig. 7.
[34]J. G. Broerman, J. Phys. Chem. Solids **32**, 1263 (1971).
[35]C. F. Lavine and A. W. Ewald, J. Phys. Chem. Solids **32**, 1121 (1971).
[36]S. H. Groves and W. Paul, in Physics of Semiconductors (Proceedings of the 7th International Conference), Dunod, Paris (Academic Press, New York, 1964).
[37]E. D. Hinkley and A. W. Ewald, Phys. Rev. **134**, A1261 (1964).
[38]O. N. Tuft and A. W. Ewald, Phys. Rev. **122**, 1431 (1961).
[39]R. P. Joshi and D. K. Ferry, Phys. Rev. B **43**, 9734 (1991).
[40]E. O. Kane, J. Phys. Chem. Solids **1**, 249 (1957).
[41]H. Ehrenreich, J. Phys. Chem. Solids **9**, 129 (1959).
[42]D. L. Rode, Phys. Rev. B **2**, 1012 (1970).
[43]D. L. Rode, Phys. Status Solidi B **55**, 687 (1973).
[44]J. S. Cetnar and D. L. Rode, J. Electron. Mater. **48**, 3399 (2019).